AMERICAN SOCIETY FOR MICROBIOLOGY | Antimicrobial Agents and Chemotherapy®

EXPERIMENTAL THERAPEUTICS

In Vivo Pharmacodynamic Characterization of a Novel Odilorhabdin Antibiotic, NOSO-502, against *Escherichia coli* and *Klebsiella pneumoniae* in a Murine Thigh Infection Model

Miao Zhao,[a,c] Alexander J. Lepak,[a] Karen Marchillo,[c] Jamie VanHecker,[c] David R. Andes[a,b,c]

[a]Department of Medicine, University of Wisconsin School of Medicine and Public Health, Madison, Wisconsin, USA

[b]Department of Medical Microbiology and Immunology, University of Wisconsin, Madison, Wisconsin, USA

[c]William S. Middleton Memorial VA Hospital, Madison, Wisconsin, USA

ABSTRACT NOSO-502 is a novel odilorhabdin antibiotic with potent activity against *Enterobacteriaceae*. The goal of these studies was to determine which pharmacokinetic/pharmacodynamic (PK/PD) indices and magnitude best correlated with efficacy in the murine thigh infection model. Six *Escherichia coli* and 6 *Klebsiella pneumoniae* isolates were utilized. MICs were determined using CLSI methods and ranged from 1 to 4 mg/liter. A neutropenic murine thigh infection model was utilized for all treatment studies. Single-dose plasma pharmacokinetics were determined in mice after subcutaneous administration of 7.81, 31.25, 125, and 500 mg/kg of body weight. Pharmacokinetic studies exhibited peak concentration (C_{max}) values of 1.49 to 84.6 mg/liter, area under the concentration-time curve from 0 h to infinity ($AUC_{0-\infty}$) values of 1.94 to 352 mg · h/liter, and beta elimination half-lives of 0.41 to 1.1 h. Dose fractionation studies were performed using total drug doses of 7.81 mg/kg to 2,000 mg/kg fractionated into regimens of every 3 h (q3h), q6h, q12h, or q24h. Nonlinear regression analysis demonstrated that AUC/MIC was the PK/PD parameter that best correlated with efficacy (R^2, 0.86). In subsequent studies, we used the neutropenic murine thigh infection model to determine the magnitude of NOSO-502 AUC/MIC needed for the efficacy against a diverse group of *Enterobacteriaceae*. Mice were treated with 4-fold-increasing doses (range, 3.91 to 1,000 mg/kg) of NOSO-502 every 6 h. The mean 24-h free-drug AUC/MIC (*f*AUC)/MIC) magnitudes associated with net stasis and 1-log kill endpoint for *K. pneumoniae* were 4.22 and 17.7, respectively. The mean *f*AUC/MIC magnitude associated with net stasis endpoint for *E. coli* was 10.4. NOSO-502 represents a promising novel, first-in-class odilorhabdin antibiotic with *in vivo* potency against *Enterobacteriaceae*.

KEYWORDS NOSO-502, *Escherichia coli*, *Klebsiella pneumoniae*, pharmacodynamics

The epidemic of antimicrobial resistance is a growing public health threat that warrants the discovery and evaluation of new antimicrobial classes. NOSO-502 belongs to a novel class of peptide antibiotics, odilorhabdins (ODLs), produced by a nonribosomal peptide synthesis (NRPS) gene cluster within the genome of *Xenorhabdus nematophila* (1). ODLs exhibit broad-spectrum activity against Gram-positive and Gram-negative pathogens, including carbapenem-resistant *Enterobacteriaceae* (CRE), by binding to the decoding center of the 16S subunit of the bacterial ribosome at a site not exploited by any known ribosome-targeting antibiotic (1). Preclinical data have shown NOSO-502 is safe and efficacious in animal models (1). The goals of our experiments were to determine the NOSO-502 pharmacokinetic/pharmacodynamic (PK/PD) index predictive of therapeutic success against *E. coli* and *K. pneumoniae* and to determine

Received 22 May 2018 **Returned for modification** 12 June 2018 **Accepted** 22 June 2018

Accepted manuscript posted online 9 July 2018

Citation Zhao M, Lepak AJ, Marchillo K, VanHecker J, Andes DR. 2018. *In vivo* pharmacodynamic characterization of a novel odilorhabdin antibiotic, NOSO-502, against *Escherichia coli* and *Klebsiella pneumoniae* in a murine thigh infection model. Antimicrob Agents Chemother 62:e01067-18. https://doi.org/10.1128/AAC.01067-18.

Address correspondence to David R. Andes, dra@medicine.wisc.edu.

For a companion article on this topic, see https://doi.org/10.1128/AAC.01016-18.

TABLE 1 *In vitro* susceptibility of NOSO-502 and strain fitness in the neutropenic thigh infection model

Organism	Median MIC (mg/liter)	Increase in burden (mean ± SD) from 0–24 h, CFU/thigh	Comment
E. coli			
ATCC 25922	4	3.28 ± 0.1	From the ATCC
6042	4	3.05 ± 0.3	TEM 10
1135	4	3.62 ± 0.3	Tet(M), ESBL
681	2	3.62 ± 0.1	ESBL
1-894-1	4	3.47 ± 0.1	Tetracycline resistant
1-741-1	4	3.13 ± 0.1	Tetracycline resistant
K. pneumoniae			
ATCC 43816	2	2.65 ± 0.1	From the ATCC
BAA 2146	1	2.64 ± 0.05	NDM-1
216	2	2.67 ± 0.1	
4105	2	2.37 ± 0.1	TEM 26, SHV-1
4110	1	2.98 ± 0.3	TEM 10, SHV-1
81-1260A	1	3.54 ± 0.1	CTX-M3, AmpC

the PK/PD index magnitude associated with stasis and bactericidal outcomes in the murine neutropenic thigh model.

RESULTS

***In vitro* susceptibility testing.** The median MIC results for NOSO-502 are shown in Table 1. The MIC range for NOSO-502 was narrow for the pathogen group, varying only 4-fold despite using a broad subset of clinical strains with demonstrated phenotypes and genotypes for resistance to other agents. Consistent with a novel mechanism, the NOSO-502 MIC results were not affected by beta-lactam or tetracycline resistance mechanisms.

Drug pharmacokinetics. Single-dose plasma pharmacokinetics of NOSO-502 following subcutaneous administration are shown in Fig. 1. NOSO-502 drug concentrations increased in a dose-dependent manner across the dose range. Peak concentrations (C_{max}s) ranged from 1.49 to 84.6 mg/liter. Area under the concentration-time curve from 0 h to infinity ($AUC_{0-\infty}$) values ranged from 1.94 to 352 mg · h/liter and were

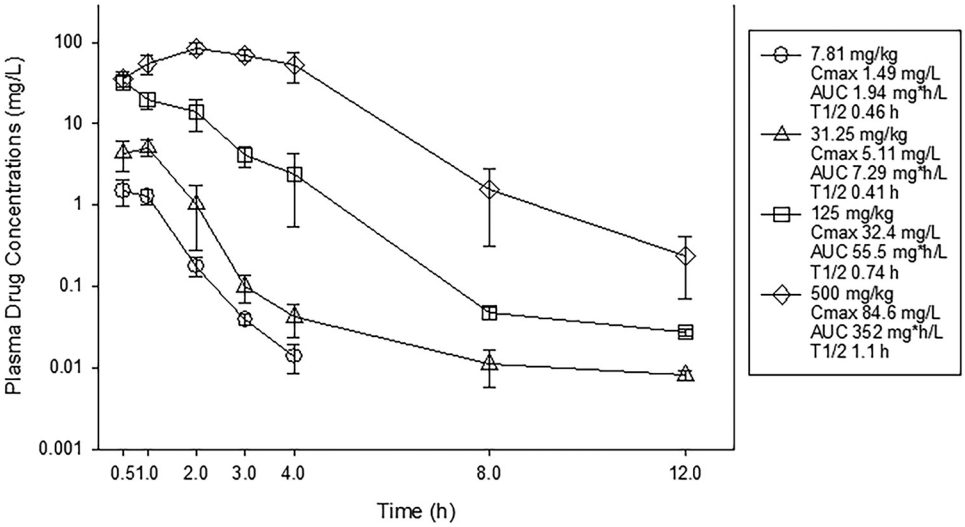

FIG 1 Single-dose plasma pharmacokinetics of NOSO-502. Four different doses that varied 4-fold on a milligram-per-kilogram basis were administered to mice by the subcutaneous route. Groups of three mice were sampled for each time point. Each symbol represents the mean from three animals; error bars show SDs. Shown in the symbol key are the maximum plasma concentration (C_{max}), the area under the concentration curve from 0 h to infinity ($AUC_{0-\infty}$), and the beta elimination half-life ($t_{1/2}$).

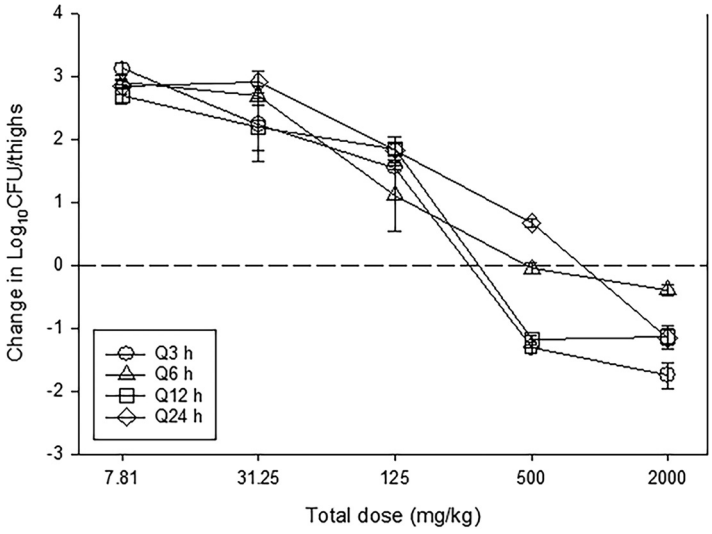

FIG 2 *In vivo* dose fractionation with NOSO-502 using a neutropenic mouse thigh model. Each symbol represents the mean from four thighs infected with *E. coli* ATCC 25922. The error bars represent the SDs. The burden of organisms was measured at the start and end of therapy. Five total drug (milligrams per kilogram per 24 h) dose levels were fractionated into one of four dosing regimens and are shown on the *x* axis. The *y* axis represents the change in organism burden from the start of therapy. The dashed horizontal line represents net stasis over the treatment period. Points above the line represent net growth, and points below represent net killing (bactericidal activity).

linear across the 7.81- to 500-mg/kg dosing range (R^2 of 0.99). The elimination half-life ($t_{1/2}$) ranged from 0.41 to 1.1 h.

PK/PD parameter determination. The dose-response relationships of NOSO-502 over a 256-fold range of doses, fractionated into one of four dosing intervals, against *E. coli* ATCC 25922 are shown in Fig. 2. At the start of therapy, mice had 6.70 $\pm$ 0.09 $\log_{10}$ CFU/thigh of *E. coli* ATCC 25922, and the organism burden increased 3.28 $\pm$ 0.11 $\log_{10}$ CFU/thigh from 0 to 24 h in untreated control mice. Each fractionation arm demonstrated relatively similar concentration-dependent activity as the total daily dose was escalated, with the highest doses studied resulting in net bactericidal activity. The similarity in the dose-response curves for each of the fractionated regimens usually indicates AUC/MIC as the predictive PK/PD index, as this PK/PD parameter is held relatively constant in each fractionated regimen. In contrast, C_{max} and time above MIC change proportionally (and inversely to each other) based on dose in each fractionated regimen.

The relationships between microbiologic effect and each of the pharmacodynamic indices, 24-h free-drug AUC/MIC (*f*AUC/MIC), 24 h free-drug C_{max}/MIC (fC_{max}/MIC), and the percent time that free drug concentrations exceed the MIC (%T_{MIC}) over 24 h against *E. coli* ATCC 25922 are shown in Fig. 3. The strongest relationship was observed when results were regressed using the 24-h *f*AUC/MIC index, with an R^2 value of 0.86. Regression with both the %T_{MIC} and fC_{max}/MIC resulted in weaker relationships based upon both visual inspection and R^2 values. Consideration of total or free drug levels did not appreciably impact the relationships between efficacy and PK/PD parameters (free-drug data are shown).

PK/PD magnitude determination. The dose-response relationships for treatment against each of the 6 *E. coli* and 6 *K. pneumoniae* strains in the neutropenic murine thigh model are shown in Fig. 4. The burdens at the start of therapy, growth in untreated controls (i.e., fitness), and drug effects were relatively similar for each isolate (Table 2). At the start of therapy, mice had 6.62 $\pm$ 0.23 $\log_{10}$ CFU/thigh of *E. coli*. The organisms grew 3.37 $\pm$ 0.28 $\log_{10}$ CFU/thigh in untreated control mice. The average maximal reduction in 6 *E. coli* strains with NOSO-502 treated mice compared to untreated controls was $-$4.17 $\pm$ 0.49 $\log_{10}$ CFU/thigh, and average maximum kill from 0 h was

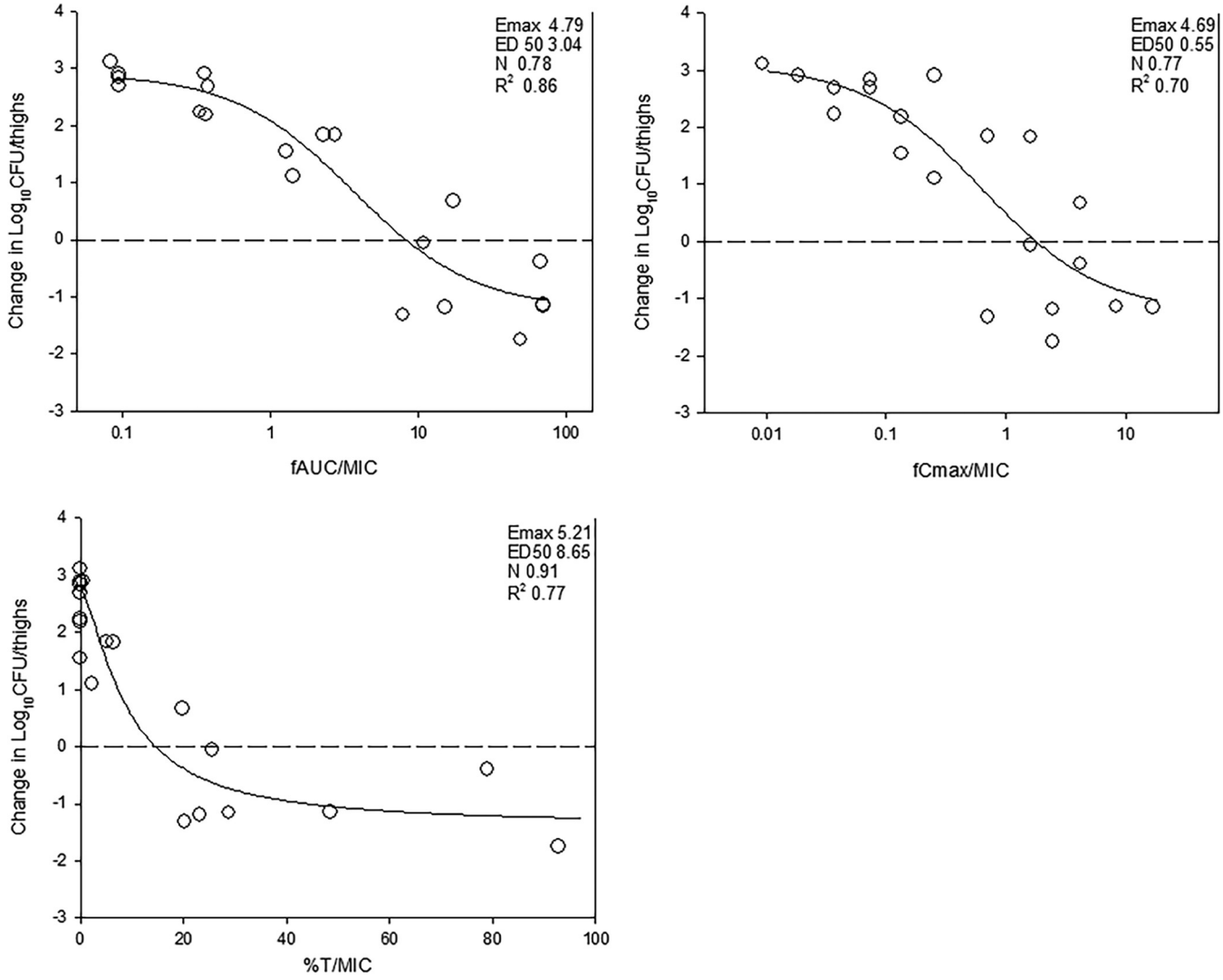

FIG 3 Impact of pharmacodynamic regression of the *in vivo* dose fractionation study with NOSO-502 against *E. coli* ATCC 25922. Each symbol represents the mean from four thighs. The dose data are expressed as free drug AUC/MIC (*f*AUC/MIC), free drug C_{max}/MIC (fC_{max}/MIC), and the percent time that plasma free drug concentrations exceeded the MIC ($\%T_{MIC}$). R^2 is the coefficient of determination. Also shown for each PD index is the maximal effect (E_{max}), the PD index value associated with 50% of the maximal effect (ED_{50}), and the slope of the relationship, or the Hill coefficient (*N*). The line drawn through the data points is the best-fit line based upon the sigmoid E_{max} formula.

-0.77 ± 0.58 $\log_{10}$ CFU/thigh. Net stasis was achieved against all strains and a $>$1-$\log_{10}$ kill against two of six strains.

The initial burden and burden increase from 0 to 24 h in untreated controls for *K. pneumoniae* were 7.12 ± 0.41 $\log_{10}$ CFU/thigh and 2.81 ± 0.40 $\log_{10}$ CFU/thigh, respectively. NOSO-502 showed slightly more potent activity against *K. pneumoniae*, with average maximal reduction compared to untreated controls at -4.43 ± 0.54 $\log_{10}$ CFU/thigh and average maximum kill from 0 h at -1.62 ± 0.64 $\log_{10}$ CFU/thigh. One-$\log_{10}$ kill was achieved against all strains and a >2 $\log_{10}$ kill against two of six strains.

The relationship between organism burden in the thigh and the plasma 24-h *f*AUC/MIC ratio is shown in Fig. 5. Calculation of the doses necessary to achieve a static and 1-$\log_{10}$ kill effect against multiple organisms is shown in Table 3. Also shown are the associated total and free-drug 24 h AUC/MIC target ratios necessary to achieve these outcomes. The mean 24-h *f*AUC/MIC values associated with net stasis endpoint for *E. coli* was 10.4. The mean 24-h *f*AUC/MIC values associated with net stasis and 1-$\log_{10}$ kill endpoints for *K. pneumoniae* were 4.22 and 17.7, respectively. The presence of antimicrobial resistance in both bacterial species did not alter the 24-h AUC/MIC

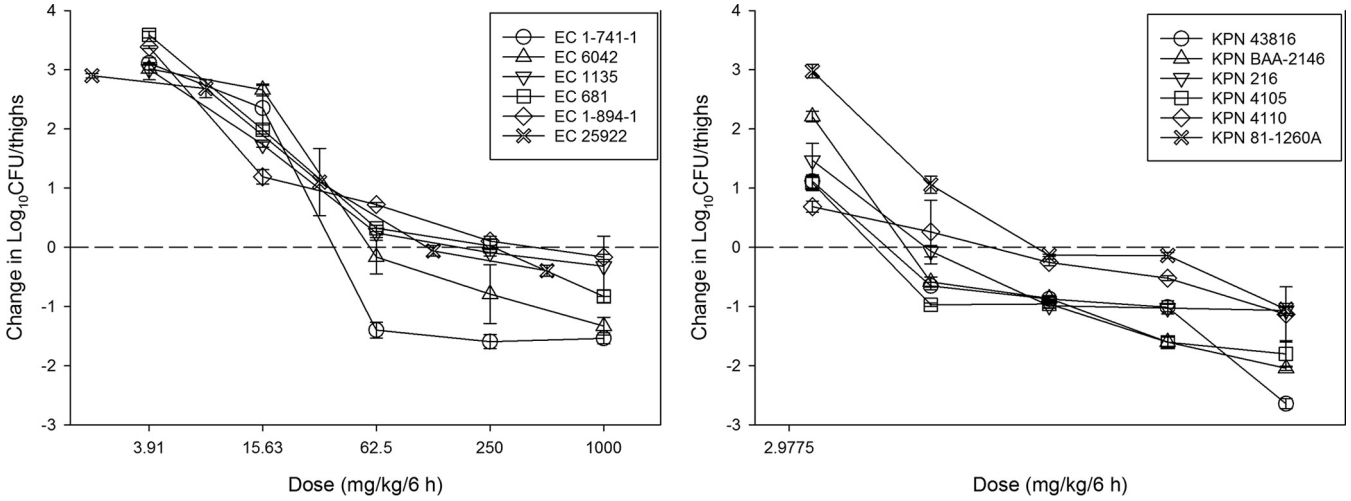

FIG 4 *In vivo* dose effect of NOSO-502 against six *E. coli* strains (left) and six *K. pneumoniae* strains (right) using a neutropenic mouse thigh model. Each symbol represents the mean from four thighs, with error bars representing SDs. Five total drug dose levels were fractionated into an every-6-h regimen. The burden of organisms was measured at the start and end of therapy. The study period was 24 h. The horizontal dashed line at 0 represents the burden of organisms in the thighs of mice at the start of therapy. Data points below the line represent killing, and points above the line represent growth.

required to produce efficacy. Additionally, while numerically lower stasis targets were observed for *K. pneumoniae* than for *E. coli*, this difference was not statistically significant (*t* test, $P = 0.08$).

DISCUSSION

The rapid spread of antibiotic resistance poses a serious threat to global public health. In recent years, carbapenem-resistant *Enterobacteriaceae* (CRE) have dramatically increased and represent an important threat to global health (2–5). The U.S. Centers for Disease Control and Prevention (CDC) has classified CRE as urgent threats (6). In response to these concerns, the development of effective antimicrobial agents, in particular novel classes, to treat these infections has been an area of intense research.

In antibiotic discovery and development, PK/PD evaluation in animal infection models plays an essential role in designing the optimal dosing regimen and planning clinical trials (7, 8). Although a drug may fail in clinical trials or for an individual patient for many reasons, one obvious potential explanatory factor is suboptimal drug exposure, which can be mitigated by optimal dosing design based on PK/PD study. In

TABLE 2 Initial burden, growth in untreated controls, and maximum kill for each organism in the *in vivo* murine thigh model[a]

Organism	Initial burden (0 h), CFU/thigh	24-h CFU/thigh in untreated controls	Maximum kill CFU/thigh (from 0 h)
E. coli			
ATCC 25922	6.70 ± 0.09	9.98 ± 0.06	−0.395 ± 0.09
6042	6.78 ± 0.28	9.83 ± 0.11	−1.33 ± 0.15
1135	6.52 ± 0.06	10.1 ± 0.23	−0.32 ± 0.51
681	6.39 ± 0.04	10.0 ± 0.06	−0.83 ± 0.10
1-894-1	6.48 ± 0.10	9.95 ± 0.08	−0.16 ± 0.04
1-741-1	6.95 ± 0.09	10.1 ± 0.05	−1.60 ± 0.12
K. pneumoniae			
ATCC 43816	7.37 ± 0.09	10.0 ± 0.03	−2.65 ± 0.09
BAA 2146	7.33 ± 0.02	9.96 ± 0.04	−2.05 ± 0.04
216	7.45 ± 0.04	10.1 ± 0.02	−1.07 ± 0.05
4105	7.35 ± 0.14	9.71 ± 0.04	−1.80 ± 0.22
4110	6.81 ± 0.37	9.80 ± 0.08	−1.14 ± 0.47
81-1260A	6.43 ± 0.08	9.98 ± 0.08	−1.05 ± 0.10

[a]Values are means ± SDs.

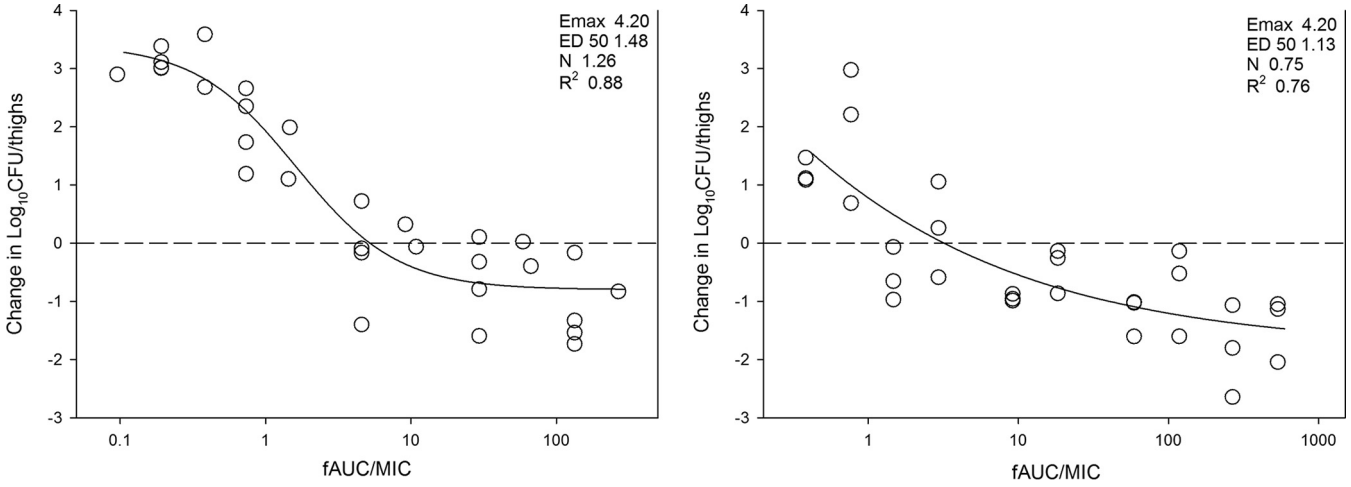

FIG 5 *In vivo* dose effect of NOSO-502 against six *E. coli* strains (left) and six *K. pneumoniae* strains (right) using a neutropenic mouse thigh model. NOSO-502 exposure is expressed as the free-drug 24-h AUC/MIC. R^2 represents the coefficient of determination. The ED_{50} represents the AUC/MIC associated with 50% of the maximal effect, and *N* is the slope of the relationship, or the Hill coefficient. The line drawn through the data points is the best-fit line based upon the sigmoid E_{max} formula. The dashed line represents the burden at the start of therapy. Points above the line represent net growth, and those below the line represent killing.

preclinical stages, PK/PD studies help define whether a drug's activity is linked optimally to concentration or time dependence. Practically, this translates into determining whether dosing regimen optimization is achieved by administering very large doses to achieve maximal concentrations in excess of the MIC or whether small, frequent doses are necessary to maintain drug concentrations above a threshold (MIC) and then maintain those concentrations for a prolonged period. Preclinical studies additionally serve to provide target drug exposures indexed to the MIC to achieve various microbiological outcomes such as net stasis or 1-$\log_{10}$ kill. These target exposures are then

TABLE 3 Pharmacodynamic targets associated with net stasis and 1-log kill in the neutropenic murine thigh model for *E. coli* and *K. pneumoniae*[a]

Organism	MIC (mg/liter)	Stasis			1-log kill		
		24-h dose (mg/kg)	24-h tAUC/MIC	24-h *f*AUC/MIC	24-h dose (mg/kg)	24-h tAUC/MIC	24-h *f*AUC/MIC
E. coli							
ATCC 25922	4	453.10	57.17	11.32	NA		
6042	4	214.67	19.45	3.85	496.0	64.37	12.74
1135	4	474.76	60.81	12.04	NA		
681	2	364.98	84.78	16.79	NA		
1-894-1	4	615.97	84.49	16.73	NA		
1-741-1	4	119.75	9.63	1.91	172.6	15.10	2.99
Mean		373.87	52.72	10.44			
Median		409.04	58.99	11.68			
SD		181.70	31.89	6.32			
K. pneumoniae							
ATCC 43816	2	55.78	6.63	1.31	276.00	54.93	10.88
BAA 2146	1	48.84	11.64	2.30	90.78	26.54	5.25
216	2	55.95	6.65	1.32	446.28	112.05	22.19
4105	2	31.53	3.79	0.75	77.72	10.57	2.09
4110	1	111.67	35.18	6.97	NA		
81-1260A	1	181.56	64.09	12.69	474.71	243.19	48.15
Mean		80.89	21.33	4.22	273.10	89.45	17.71
Median		55.87	9.14	1.81	276.00	54.93	10.88
SD		56.21	23.89	4.73	188.45	94.23	18.66

[a]tAUC/MIC, total drug AUC/MIC; *f*AUC/MIC, free drug AUC/MIC; NA, not achieved.

utilized in the context of human pharmacokinetics and MIC distribution in Monte Carlo simulations to estimate target achievement to enable rational go or no-go decision making in a relatively early stage of new antibiotic development (9, 10). In this study, we examined the PK/PD relationships and determined the magnitude associated with efficacy endpoints for a novel antibiotic NOSO-502 in an established neutropenic murine thigh infection model. NOSO-502 belongs to a novel peptide antibiotic class, the odilorhabdins (ODLs), which exhibit a number of potential advantages. Mechanistic studies have demonstrated that ODLs interfere with protein synthesis by binding to the bacterial 16S ribosomal subunit, leading to errors in translation and cell death (1). While other antibiotic classes also bind to the small ribosomal subunit (e.g., tetracyclines and aminoglycosides), the site of binding for ODLs is distinct such that there has been no evidence in preclinical studies of cross-resistance to other antibiotics that affect protein translation (1). Importantly, the activity of NOSO-502 against Gram-positive and Gram-negative bacterial pathogens, including CRE, has been demonstrated (1).

Prior *in vivo* study of ODLs showed dose-dependent response in mouse models of *E. coli* and *K. pneumoniae* septicemia, urinary tract infection (UTI), and lung infection, but only single-dose levels were studied, which precludes adequate PK/PD assessment (1). The current study represents the first traditional PK/PD evaluation of a novel ODL antibiotic, NOSO-502, using the murine thigh infection model. Using a dose fractionation study design, we found AUC/MIC to be the PK/PD index predictive of efficacy for NOSO-502. This is perhaps not unexpected given that other agents that affect protein translation have also been predominantly associated with the PK/PD index AUC/MIC. For example, the PK/PD indices for tetracycline class agents, such as tetracycline (11), minocycline (12), tigecycline (13), eravacycline (14), and omadacycline (15), have been shown to be AUC/MIC.

Our multiorganism PK/PD target studies performed with NOSO-502 demonstrated very similar dose-dependent activity, with net static activity against all strains. Given the relatively narrow MIC distribution, this similarity was expected. This also demonstrated that similar to the previous *in vitro* evaluations, resistance mechanisms to beta-lactams and tetracyclines did not appreciably affect the *in vivo* pharmacodynamic activity. A limitation to the current study is that we did not use any strains with known aminoglycoside resistance mechanisms.

We did observe enhanced activity of NOSO-502 against *K. pneumoniae*, as approximately 4-fold less drug was needed (i.e., dose-response curves shifted to the left) for stasis and bactericidal endpoints compared to those for *E. coli*. We also observed, similar to previous studies (data provided by sponsor and not shown), enhanced *in vitro* effects against *K. pneumoniae*, with numerically lower MICs for most *K. pneumoniae* strains. However, the difference in MIC was only 2-fold between *K. pneumoniae* and *E. coli*. This resulted in free 24-h AUC/MIC targets that were roughly 2-fold lower for *K. pneumoniae* than for *E. coli*, but this difference was not statistically significant. A killing endpoint (1-log kill) was achieved for *K. pneumoniae* at approximately 4-fold the stasis target; however, it should be noted that we did not achieve a large number of 1-log kill endpoints against *E. coli* in order to make similar comparisons for this endpoint.

In conclusion, these studies demonstrated that NOSO-502 exhibits dose-dependent *in vivo* activity against *K. pneumoniae* and *E. coli* strains, including those with mechanisms of resistance to beta-lactams and tetracyclines. It is a promising novel antibiotic from the newly discovered odilorhabdin class. AUC/MIC was the PK/PD index that best predicted efficacy, and we were able to demonstrate both net stasis and bactericidal endpoints in a clinically relevant animal infection model. The PD index and targets identified in this study will be useful in guiding appropriate dosing regimen design for future clinical studies in the context of human pharmacokinetic exposures and MIC distribution. Further development and studies are warranted, especially in light of the urgent need for novel drugs to address the rise of drug resistant infections.

MATERIALS AND METHODS

Organisms, media, and antibiotic. Six *E. coli* and 6 *K. pneumoniae* strains were used for these studies (Table 1). The strains were chosen to include common tetracycline and beta-lactam resistance phenotypes. They were grown, subcultured, and quantified using Mueller-Hinton broth (MHB) and agar (Difco Laboratories, Detroit, MI). NOSO-502 for *in vitro* and *in vivo* studies was supplied by the study sponsor (Nosopharm SAS, Nîmes, France). The compound was prepared by reconstitution in sterile water to pH 5.5 to 6.5 and subsequent dilution in sterile 5% D-mannitol solution.

***In vitro* susceptibility testing.** The MICs of NOSO-502 for the various isolates were determined using Clinical and Laboratory Standards Institute (CLSI) microdilution methods (16, 17). All MIC assays were performed in duplicate on three separate occasions. The median MIC of replicate assays is reported and was utilized in PK/PD analyses.

Murine thigh infection model. Animals for the present studies were maintained in accordance with criteria of the Association for Assessment and Accreditation of Laboratory Animal Care International (AAALAC). All animal studies were approved by the Animal Research Committee of the William S. Middleton Memorial Veterans Hospital. Six-week-old, specific-pathogen-free, female ICR/Swiss mice weighing 23 to 27 g were used for all studies (Harlan Sprague-Dawley, Indianapolis, IN). Mice were rendered neutropenic (neutrophils, $<100/mm^3$) by injecting them with cyclophosphamide (Mead Johnson Pharmaceuticals, Evansville, IN) subcutaneously 4 days (150 mg/kg) and 1 day (100 mg/kg) before thigh infection. Previous studies have shown that this regimen produces neutropenia in this model for 5 days (18). Broth cultures of freshly plated bacteria were grown to logarithmic phase overnight to an absorbance of 0.3 at 580 nm (Spectronic 88; Bausch and Lomb, Rochester, NY). After a 1:10 dilution into fresh Mueller-Hinton broth, bacterial counts of the inoculum ranged from $10^{7.1}$ to $10^{7.4}$ CFU/ml. Thigh infections with each of the isolates were produced by injection of 0.1 ml of inoculum into the thighs of isoflurane-anesthetized mice. NOSO-502 therapy was initiated 2 h after the infection procedure. After 24 h, the animals were euthanized and thighs aseptically removed, homogenized, and plated for CFU determination. No treatment and 0-h controls were included in all experiments. Four thigh replicates were included for all treatment and control groups.

Drug pharmacokinetics. Single-dose plasma pharmacokinetics of NOSO-502 in mice were analyzed. Animals were administered single subcutaneous doses (0.2 ml/dose) of NOSO-502 at dose levels of 7.81, 31.25, 125, and 500 mg/kg. Groups of three mice were sampled at each time point (seven time points, consisting of 0.5, 1, 2, 3, 4, 8, and 12 h) and dose level. Samples were then centrifuged for 5 min at 4,000 rpm, and plasma was removed and frozen at −20°C until assay. Plasma concentrations were determined using liquid chromatography-tandem mass spectrometry (LC-MS/MS) by the sponsor. The lower limit of detection of the LC-MS/MS was 7.2 ng/ml. Pharmacokinetic parameters, including elimination half-life ($t_{1/2}$), area under the concentration-time curve ($AUC_{0-\infty}$), and peak concentrations (C_{max}), were calculated using a noncompartmental model. The beta $t_{1/2}$ was determined by linear least-squares regression. The $AUC_{0-\infty}$ was calculated from the mean concentrations using the trapezoidal rule. Pharmacokinetic estimates for dose levels that were not directly measured were calculated using linear interpolation for dose levels between those with measured kinetics and linear extrapolation for dose levels above or below the highest and lowest dose levels with kinetic measurements. A plasma protein binding of 80.2% was used in the current study to calculate free drug concentrations for analysis based upon prior unpublished data from the sponsor.

PK/PD parameter determination. A dose fractionation study was undertaken to determine the PK/PD index (AUC/MIC, C_{max}/MIC, or $\%T_{MIC}$) that was predictive of efficacy for NOSO-502. Fourfold increasing doses (range, 7.81 mg/kg to 2,000 mg/kg) of NOSO-502 were fractionated into dosing regimens of every 3 h (q3h), q6h, q12h, and q24h. Mice were infected with isolate ATCC 25922 as described above and administered NOSO-502 by subcutaneous injection according to the dosing regimen prescribed in the fractionation design. After 24 h, the mice were euthanized and CFU count in the thighs was determined. To determine which PK/PD index was most closely linked with efficacy, the number of bacteria in the thigh at the end of 24 h of therapy was correlated with (i) the free C_{max}/MIC ratio (fC_{max}/MIC), (ii) the 24-h free AUC/MIC ratio (*f*AUC/MIC), and (iii) the percentage of the dosing interval during which plasma free drug levels exceeded the MIC for each of the dosage regimens studied ($\%T_{MIC}$). The correlation between efficacy and each of the three PK/PD indices was determined by nonlinear least-squares multivariate regression (SigmaPlot version 13.0; Systat Software, San Jose, CA). The model is derived from the Hill equation. The coefficient of determination (R^2) was used to estimate the variance that might be due to regression with each of the PK/PD indices.

PK/PD parameter magnitude studies. Dose-response experiments using the thigh model were performed for six *E. coli* isolates as described above. The dose range consisted of 4-fold increases (range, 3.91 to 1,000 mg/kg/6 h) in drug concentration with administration by the subcutaneous route. The dose-response relationships were quantified and the relationship between the PK/PD parameter AUC/MIC and treatment efficacy using the sigmoid E_{max} (Hill) model was determined using Sigma Plot version 13.0, Systat Software, San Jose, CA. These PK/PD relationships were examined utilizing the plasma total and free drug concentrations from pharmacokinetic studies. The coefficient of determination (R^2) from this model was used to numerically quantify the strength of this relationship. This coefficient represents the percentage of the variance in bacterial numbers that can be attributed to the PK/PD parameter. The doses required for a static effect (static dose) and 1-log kill (1 log-kill dose) compared to the start of therapy for multiple *E. coli* and *K. pneumoniae* pathogens in the thigh model were determined utilizing the plasma total and free drug concentrations using the following equation:

$$\log_{10} D = \frac{\log_{10}[E/(E_{max} - E)]}{N} + \log \mathrm{ED}_{50}$$

where E is the growth from 0 h, E_{max} is the maximum effect, ED_{50} is the dose required to achieve 50% of the E_{max}, N is the slope of the dose-effect curve, and D is the dose required to achieve net stasis. For 1-log kill, E was set to growth from 0 h plus 1 in order to calculate dose (D) for 1-log kill. The associated 24-h total and free drug AUC/MIC targets for each organism were calculated.

ACKNOWLEDGMENTS

This study was funded by Nosopharm SAS, Nîmes, France.
Funded by NOSO.

REFERENCES

1. Pantel L, Florin T, Dobosz-Bartoszek M, Racine E, Sarciaux M, Serri M, Houard J, Campagne JM, de Figueiredo RM, Midrier C, Gaudriault S, Givaudan A, Lanois A, Forst S, Aumelas A, Cotteaux-Lautard C, Bolla JM, Vingsbo Lundberg C, Huseby DL, Hughes D, Villain-Guillot P, Mankin AS, Polikanov YS, Gualtieri M. 2018. Odilorhabdins, antibacterial agents that cause miscoding by binding at a new ribosomal site. Mol Cell 70:83–94.e7. https://doi.org/10.1016/j.molcel.2018.03.001.
2. Potter RF, D'Souza AW, Dantas G. 2016. The rapid spread of carbapenem-resistant Enterobacteriaceae. Drug Resist Updat 29:30–46. https://doi.org/10.1016/j.drup.2016.09.002.
3. van Duin D, Doi Y. 2017. The global epidemiology of carbapenemase-producing Enterobacteriaceae. Virulence 8:460–469. https://doi.org/10.1080/21505594.2016.1222343.
4. Friedman ND, Carmeli Y, Walton AL, Schwaber MJ. 2017. Carbapenem-resistant Enterobacteriaceae: a strategic roadmap for infection control. Infect Control Hosp Epidemiol 38:580–594. https://doi.org/10.1017/ice.2017.42.
5. Trecarichi EM, Tumbarello M. 2017. Therapeutic options for carbapenem-resistant Enterobacteriaceae infections. Virulence 8:470–484. https://doi.org/10.1080/21505594.2017.1292196.
6. Centers for Disease Control and Prevention. 2013. Antibiotic resistance threats in the United States, 2013. Centers for Disease Control and Prevention, Atlanta, GA. https://www.cdc.gov/drugresistance/threat-report-2013/index.html. Accessed 30 April 2018.
7. Andes DR, Lepak AJ. 2017. In vivo infection models in the pre-clinical pharmacokinetic/pharmacodynamic evaluation of antimicrobial agents. Curr Opin Pharmacol 36:94–99. https://doi.org/10.1016/j.coph.2017.09.004.
8. Craig WA. 1998. Pharmacokinetic/pharmacodynamic parameters: rationale for antibacterial dosing of mice and men. Clin Infect Dis 26:1–10; quiz, 11–12. https://doi.org/10.1086/516284.
9. Andes D, Craig WA. 2002. Animal model pharmacokinetics and pharmacodynamics: a critical review. Int J Antimicrob Agents 19:261–268. https://doi.org/10.1016/S0924-8579(02)00022-5.
10. Ambrose PG. 2008. Use of pharmacokinetics and pharmacodynamics in a failure analysis of community-acquired pneumonia: implications for future clinical trial study design. Clin Infect Dis 47:S225–S231. https://doi.org/10.1086/591427.
11. Agwuh KN, MacGowan A. 2006. Pharmacokinetics and pharmacodynamics of the tetracyclines including glycylcyclines. J Antimicrob Chemother 58:256–265. https://doi.org/10.1093/jac/dkl224.
12. Zhou J, Ledesma KR, Chang KT, Abodakpi H, Gao S, Tam VH. 2017. Pharmacokinetics and pharmacodynamics of minocycline against *Acinetobacter baumannii* in a neutropenic murine pneumonia model. Antimicrob Agents Chemother 61:e02371-16. https://doi.org/10.1128/AAC.02371-16.
13. Rubino CM, Bhavnani SM, Forrest A, Dukart G, Dartois N, Cooper A, Korth-Bradley J, Ambrose PG. 2012. Pharmacokinetics-pharmacodynamics of tigecycline in patients with community-acquired pneumonia. Antimicrob Agents Chemother 56:130–136. https://doi.org/10.1128/AAC.00277-10.
14. Zhao M, Lepak AJ, Marchillo K, VanHecker J, Andes DR. 2017. *In vivo* pharmacodynamic target assessment of eravacycline against *Escherichia coli* in a murine thigh infection model. Antimicrob Agents Chemother 61:e00250-17. https://doi.org/10.1128/AAC.00250-17.
15. Lepak AJ, Zhao M, Marchillo K, VanHecker J, Andes DR. 2017. *In vivo* pharmacodynamic evaluation of omadacycline (PTK 0796) against *Streptococcus pneumoniae* in the murine pneumonia model. Antimicrob Agents Chemother 61:e02368-16. https://doi.org/10.1128/AAC.02368-16.
16. Clinical and Laboratory Standards Institute. 2015. Methods for dilution antimicrobial susceptibility tests for bacteria that grow aerobically; approved standard—10th ed. CLSI document M07-A10. Clinical and Laboratory Standards Institute, Wayne, PA.
17. Clinical and Laboratory Standards Institute. 2015. Performance standards for antimicrobial susceptibility testing; 25th informational supplement. CLSI document M100-S25. Clinical and Laboratory Standards Institute, Wayne, PA.
18. Leggett JE, Fantin B, Ebert S, Totsuka K, Vogelman B, Calame W, Mattie H, Craig WA. 1989. Comparative antibiotic dose-effect relations at several dosing intervals in murine pneumonitis and thigh-infection models. J Infect Dis 159:281–292. https://doi.org/10.1093/infdis/159.2.281.